IET Communications

Research Article

Relevant support recovery algorithm in modulated wideband converter

ISSN 1751-8628
Received on 4th June 2018
Revised 31st October 2018
Accepted on 4th July 2019
E-First on 8th October 2019
doi: 10.1049/iet-com.2018.5474
www.ietdl.org

Jiawei Zhu[1], *Jie Li*[2], *Jian Li*[1], *Zhi Li*[1] ✉
[1]*Department of Electronics and Information Engineering, Sichuan University, Chengdu, People's Republic of China*
[2]*Department of Computer Science, Beijing University of Posts and Telecommunications, Beijing, People's Republic of China*
✉ *E-mail: lizhi@scu.edu.cn*

Abstract: Modulated wideband converter (MWC) is a compressed spectrum sensing system that randomly moves the sparse wideband signal spectrum to the baseband to realise low-speed sampling. Then, obtaining the effective support which is based on compressed sensing is the most important part for the signal recovery from samples. Aimed at the poor anti-noise performance of the support recovery, a relevant support recovery algorithm (RSRA) is proposed in modulated wideband converter for spectrum sensing. Specifically, the optimal initial support index is obtained by least squares. Then, the correlation between the measurement matrix column vector corresponding to the adjacent index and the sampling matrix is calculated, and the adjacent index with larger correlation is added to the support. The whole support is acquired by iterative updating under the thought of matching pursuit. Being different from other algorithms, RSRA takes the correlation about adjacent indexes into account, which can weaken the noise interference. Theoretical analysis and numerical simulations show that the proposed scheme can improve the recovery rate of effective support in lower SNR. While improving the anti-noise capability, other aspects of performance such as channels number and sparsity will not be sacrificed.

1 Introduction

Spectrum sensing is a key technology of cognitive radios. It can detect the occupancy of the spectrum and thus achieve dynamic spectrum access and maximise the utilisation of spectrum resources. The popular spectrum sensing methods include energy detection, matched filter detection, and cyclostationary detection. However, the above spectrum detection technologies are all applied to the field of low-frequency sensing. In terms of radio frequency (RF) signal processing, they will be limited and have poor performance on spectrum sensing. Spectrum sensing is an indispensable part of electromagnetic spectrum detection technology.

As the bandwidth occupied by electromagnetic signals becomes wider, the traditional Nyquist sampling theorem can hinder the development of hardware processing technologies such as analogue-to-digital converters and digital signal processing. With the electromagnetic environment becoming increasingly complex [1], conventional wideband digital receivers have met more and more challenges, including high sampling rates, complex structures, and cross-channel signal problems [2]. The multi-coset sampling based on the periodic non-uniform sampling was proposed in [3], which can realise sub-Nyquist sampling under certain conditions and can reconstruct the original signal accurately from the sampling. However, the exact phase shift of the sampling clock is not easy to be controlled precisely and requires more prior knowledge. Fortunately, compressed sensing (CS) technique [4, 5] proposed by Donoho D L. effectively breaks the limitations of traditional Nyquist sampling and reconstructs the original signal with a small number of samples. Therefore, the direct compression sampling technique in the time domain becomes the focus of the further research [6–8]. The article [9, 10] proposed the random demodulator (RD) to obtain the compressed sample sequence, which mixes the signal and the pseudo-random sequence, and the output is integrated and sampled at a fixed rate. Finally, the original signal can be recovered by the compressed sampling sequence combined with recovery algorithms of CS. However, the RD is mainly for the multi-tone signal. The research showed that RD is more sensitive to the signal model. In addition, if the sparse multi-band signal is sampled at sub-Nyquist rate using the RD, the frequency domain requires to be discretised. When the frequency resolution is lower, the reconstruction error becomes larger. Then, the dimension of the sampling matrix will be increased when the resolution is high, which can result in heavy workload. The carrier frequency is unknown so that the traditional coherent demodulation method and the periodic non-uniform sampling method are incapable in these application scenarios. Subsequently, Eldar Y C. and her team proposed the modulated wideband converter (MWC) based on the CS [11, 12], which actually achieved a significant breakthrough about under-sampling in the analogue domain. MWC can effectively reduce the sampling rate and directly sample the RF signal. Then, it also can recover the blind sparse multi-band signal effectively without the priori knowledge of spectrum position, so it has the unique advantage in full band monitoring and reconnaissance.

The under-sampling data retains the characteristic information of the original signal. However, since the sampling data is discretised, it is necessary to realise the signal reconstruction by processing the discrete samples. The whole signal recovery process for MWC includes support recovery and signal reconstruction, in which support recovery plays a pivotal role. The reduce and boost algorithm (ReMBo) [13] converted infinite measurement vectors randomly into a single measurement vector to realise the signal recovery. Subsequently, the continuous-to-finite framework (CTF) was proposed to reconstruct the support and the recovery algorithm was orthogonal matching pursuit (MMV-OMP) [11]. In [14], the RPMB algorithm was inspired by ReMBo, which further improved the recovery rate of the support. It converted infinite measurement vectors into a multiple measurement vector with a random matrix. The improved algorithm based on modulated wideband converter (IOMP) was proposed in [15] to boost the recovery rate with less samples. The articles in [16, 17] put forward the sparse multi-band signal recovery algorithm to reduce the hardware complexity, which can use fewer sampling channels to recover the original signal under the same recovery performance. [18] presented distributed modulation wideband converter (DMWC) to achieve spectrum detection, which can change multi-channels single-node into multi-nodes single-channel flexibly to solve the defect of non-adjustable numbers of hardware channel. In [19, 20], they proposed to arrange sensing nodes in a linear array to realise the spectrum

© The Institution of Engineering and Technology 2019

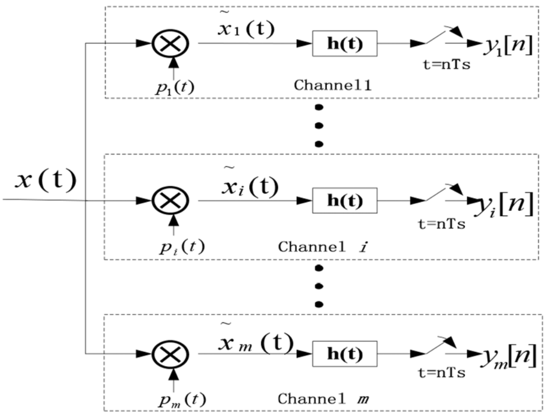

Fig. 1 *MWC sampling process*

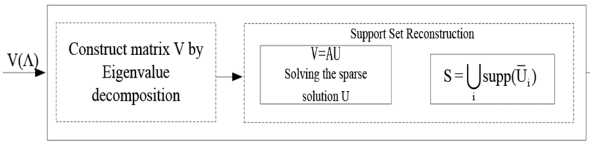

Fig. 2 *Module of CTF*

sensing. However, in the case of lower SNR, the support recovery performance of the above algorithms are relatively lower.

MWC is introduced as a means of spectrum sensing, in which the recovery support can provide the spectrum occupancy. The support is the set of locations of the carrier band within the wide band. Due to the unavoidable noise, the reconstructed support will be identified incorrectly, which will affect the accuracy of spectrum sensing. Boosting the recovery performance under low signal-to-noise ratio has been a challenge for MWC. Therefore, combined with the characteristics of the sparse multi-band model, a relevant support recovery algorithm (RSRA) is proposed based on MWC for spectrum sensing to reduce the impact of the noise. The initial support set is determined using the idea of the least squares method, and then to select the valid adjacent support index which has large correlation with sampling matrix to improve the recognition rate of support. The correlation between the adjacent indexes of the initial support set plays a vital role in reconstructing the original signal. Compared with the other algorithms under several conditions, simulation results demonstrate that RSRA for MWC to recover the signal is feasible in time domain and frequency domain, and has better anti-noise performance than other algorithms.

2 MWC model for spectrum sensing

2.1 Sampling

The MWC sampling process for sparse multiband signal is shown in Fig. 1. The system contains m sampling channels. The signal enters into the channels simultaneously, and passes through a mixer $p_i(t)$, a low-pass filter $h(t)$, and a low-speed analogue-to-digital conversion independently. The output is the compressive sampling sequence. The system exploits spread-spectrum techniques, and the mixer aliases the spectrum, such that a spectrum portion from each band appears in baseband. After mixing, the signal spectrum is truncated by the low-pass filter $h(t)$ so that the sampling rate of channels is sufficiently low.

In the MWC sampling system, the ith mixer expressed by $p_i(t)$ is chosen as a piecewise constant T_p -periodic function that alternates between the levels ± 1 for each of M equal time intervals. The form of Fourier series is:

$$p_i(t) = \sum_{l=-\infty}^{\infty} c_{il} \mathrm{e}^{j(2\pi/T_p)lt} \tag{1}$$

where c_{il} represents the Fourier coefficient of $p_i(t)$. The Fourier transform of $\tilde{x}_i(t) = x(t)p_i(t)$ passing through the analogue multiplier is:

$$X_i(f) = \int_{-\infty}^{\infty} \tilde{x}_i(t)\mathrm{e}^{-j2\pi ft}\mathrm{d}t \simeq \sum_{-\infty}^{+\infty} c_{il} X(f - lf_p) \tag{2}$$

Thus, $X_i(f)$ is the result of the linear shift in f_p about the original input signal spectrum $\boldsymbol{X}(f)$. After moving the spectrum, the baseband will contain all the frequency band information. After the low rate sampling, the discrete-time Fourier transform of the compressed sample sequence $y_i[n]$ is expressed as:

$$\begin{aligned} Y_i\left(\mathrm{e}^{j2\pi f\mathrm{T}_s}\right) &= \sum_{n=-\infty}^{n=\infty} y_i[n]\mathrm{e}^{-j2\pi fn\mathrm{T}_s} \\ &= \sum_{l=-L_0}^{+L_0} c_{il} X(f - lf_p), f \in F_s \end{aligned} \tag{3}$$

L_0 is about half of the number of partitioned $X(f)$. Then, it is calculated by follows [11]:

$$-\frac{f_s}{2} + (L_0 + 1)f_p \geq \frac{f_{\mathrm{nyq}}}{2} \Rightarrow L_0 = \frac{f_{\mathrm{nyq}} + f_s}{2f_p} - 1 \tag{4}$$

where f_s is the sub-sampling rate, f_{Nyq} is the Nyquist rate. Then, $f_p = 1/T_p$.

Combining the MWC sampling form with the CS theory, (3) can be converted to the following:

$$\boldsymbol{y}(f) = \mathrm{A}\mathrm{Z}(f) \tag{5}$$

In (3), the coefficient c_{il} constitutes the matrix $\boldsymbol{A}$. Then, the dimension of $\boldsymbol{A}$ is $m \times L$. $\boldsymbol{Y}(f)$ is an m-dimensional vector, and its ith element is $y_i(f) = Y_i\left(\mathrm{e}^{j2\pi f\mathrm{T}_s}\right)$. $\boldsymbol{Z}(f)$ is the representation of the signal to be recovered from $\boldsymbol{Y}(f)$, and $\boldsymbol{Z}(f)$ is unknown. Following is the relationship between $\boldsymbol{X}(f)$ and $\boldsymbol{Z}(f)$:

$$z_i(f) = X(f + (i - L_0 - 1)f_p), 1 \leq i \leq L \tag{6}$$

where $L = 2L_0 + 1$.

2.2 Reconstruction

MWC signal reconstruction process can be summarised as using the low-speed sampling sequence $\boldsymbol{y}[n]$ to recover the original multi-band signal $\boldsymbol{x}[n]$. Further, it can be attributed to the process of recovering $\boldsymbol{Z}(f)$ from $\boldsymbol{Y}(f)$. The recovery support in MWC can provide the occupation of the spectrum. The support is the set of locations of the carrier band within the wide band. Due to the mixer with random moving, the sub-bands that spread throughout the whole frequency domain all move into the baseband range. So, the support recovery is an important stage for MWC in realising the spectrum detection. The article [11] used a CTF module to obtain the support. The recovery processing contains several main steps as shown in Fig. 2. The CTF module contains the eigenvalue decomposition and the support reconstruction. The purpose of eigenvalue decomposition is to drastically reduce the dimension of the sampling matrix while maintaining the sampling characteristics.

Specifically, obtain the matrix $\boldsymbol{Q}$ by (7).

$$\boldsymbol{Q} = \int \boldsymbol{y}(f)\boldsymbol{y}^H(f)\mathrm{d}f \simeq \sum_{n=-\mathrm{L}_0}^{L_0} \boldsymbol{y}[n]\boldsymbol{y}^{\mathrm{T}}[n] \tag{7}$$

where $\boldsymbol{y}[n] = [y_1[n], \ldots, y_m[n]]^T$ is the sampling vector sampled at time interval nT_s. The dimension of $\boldsymbol{Q}$ is $\mathrm{m} \times \mathrm{m}$. Decompose the

© The Institution of Engineering and Technology 2019

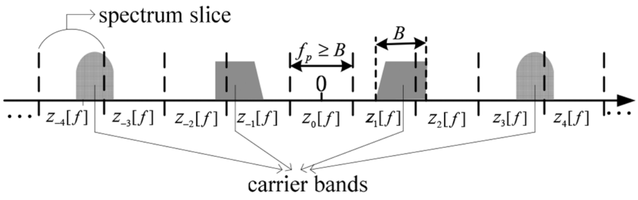

Fig. 3 *Sparse broadband signal model*

matrix $\boldsymbol{Q}$ according to (8), and matrix $\boldsymbol{V}$ is the decomposed matrix constructed from matrix $\boldsymbol{Q}$ [11].

$$\boldsymbol{Q} = \boldsymbol{P}\Lambda\boldsymbol{P}^H = \text{VV}^H \tag{8}$$

The support reconstruction is actually a sparse solution process. The final support $\boldsymbol{S} = supp(\boldsymbol{U})$ can be obtained by solving the sparsest solution of the (9):

$$\min \| \boldsymbol{U} \|_1 \text{ s.t. } \boldsymbol{V} = \text{AU} \tag{9}$$

where $\boldsymbol{U}$ in (9) is an unknown vector that is the substitution of $\boldsymbol{Z}(f)$ in (5), and $\boldsymbol{U}$ has the same support with $\boldsymbol{Z}(f)$. The solutions of $\boldsymbol{U}$ are not unique. We want to solve the sparsest vector $\boldsymbol{U}$ which satisfied $\boldsymbol{V} = \text{AU}$. The reconstructed support of the original signal by solving the sparse solution will be introduced in the next section.

In most cases, the original signal represented in frequency domain can achieve the purpose for signal perception, without focusing on the specific form of the time domain. Based on this feature, how to obtain the signal support is the key to realise the spectrum sensing.

If necessary, the original signal can be recovered by solving the following formula (9):

$$\begin{cases} z_i[n] = \boldsymbol{A}_s^{\dagger}\boldsymbol{y}[n],\ i \in S \\ z_i[n] = 0,\ i \notin S \end{cases} \tag{10}$$

where $\boldsymbol{A}_S^{\dagger}$ is the pseudo-inverse of $\boldsymbol{A}_S$, and $\boldsymbol{A}_S$ contains the columns of $\boldsymbol{A}$ indexed by $\boldsymbol{S}$. Then, $z_i[n]$ is the inverse-discrete time Fourier transform (DTFT) of $z_i(f)$.

3 RSRA algorithm

The recovery support in MWC can provide the occupation of the spectrum. Due to the mixer spreading the original signal spectrum randomly over the whole wideband, the reconstruction of the correct support set is more sensitive to noise. So, reducing the impact of noise is extremely important for MWC recovery.

Inspired by the sparse multi-band signal model, we analysed the traditional signal reconstruction algorithm combined the MWC under-sampling process. For the under-sampling process of MWC, the entire frequency band is divided into L spectral slices, and each spectrum slice is shifted to the baseband by $\text{l}f_p$ with $l \in [1, L]$. Finally, low speed sampling is carried out in the baseband which is well below the Nyquist bandwidth. The back end uses the CS recovery algorithm reconstruct the spectral support, which represents the location of the non-zero spectrum slice. As shown in Fig. 3, each carrier band occupies up to two consecutive spectrum slices due to the continuity of the band, and one part of the slice often contains more carrier energy than its adjacent slice. B in Fig. 3 represents the maximum width among all carrier bands. The support that contains the more energetic spectrum can be identified easily when solving the sparse solution.

In the CTF module, since the support of $\boldsymbol{U}$ is the same as the support of signal $\boldsymbol{Z}(f)$, the spectral support is obtained directly by calculating the sparsest solution $\boldsymbol{U}$ of $\boldsymbol{V} = \text{AU}$. Accordingly, the matrix $\boldsymbol{U}$ also needs to be updated iteratively, so matrix $\boldsymbol{R}$ is introduced as the residual matrix. Since the support is obtained by constantly updating in this process, the residual matrix $\boldsymbol{R}$ needs to be updated to reflect the difference between the supports as follows:

$$\begin{cases} \hat{\boldsymbol{U}} = \boldsymbol{A}_S^{\dagger}\boldsymbol{V} = \left(\boldsymbol{A}_S^{\text{T}}\boldsymbol{A}_S\right)^{-1}\boldsymbol{A}_S^{\text{T}}\boldsymbol{V} \\ \boldsymbol{R} = \boldsymbol{V} - \boldsymbol{A}_S\hat{\boldsymbol{U}} \end{cases} \tag{11}$$

The measurement matrix $\boldsymbol{A}$ and the residual matrix $\boldsymbol{R}$ are shown in (12) and (13):

$$\boldsymbol{A} = \begin{bmatrix} \boldsymbol{a}_{11} & \cdots & \boldsymbol{a}_{1q} & \cdots & \boldsymbol{a}_{1i} & \cdots & \boldsymbol{a}_{1l} \\ \vdots & & \vdots & & \vdots & & \vdots \\ \boldsymbol{a}_{r1} & \cdots & \boldsymbol{a}_{\text{rq}} & \cdots & \boldsymbol{a}_{\text{ri}} & \cdots & \boldsymbol{a}_{\text{rl}} \\ \vdots & & \vdots & & \vdots & & \vdots \\ \boldsymbol{a}_{m1} & \cdots & \boldsymbol{a}_{\text{mq}} & \cdots & \boldsymbol{a}_{\text{mi}} & \cdots & \boldsymbol{a}_{\text{ml}} \end{bmatrix} \tag{12}$$

$$\boldsymbol{R} = \begin{bmatrix} \boldsymbol{r}_{11} & \cdots & \boldsymbol{r}_{1q} & \cdots & \boldsymbol{r}_{1i} & \cdots & \boldsymbol{r}_{1l} \\ \vdots & & \vdots & & \vdots & & \vdots \\ \boldsymbol{r}_{r1} & \cdots & \boldsymbol{r}_{\text{rq}} & \cdots & \boldsymbol{r}_{\text{ri}} & \cdots & \boldsymbol{r}_{\text{rl}} \\ \vdots & & \vdots & & \vdots & & \vdots \\ \boldsymbol{r}_{m1} & \cdots & \boldsymbol{r}_{\text{mq}} & \cdots & \boldsymbol{r}_{\text{mi}} & \cdots & \boldsymbol{r}_{\text{ml}} \end{bmatrix} \tag{13}$$

The expression of $\boldsymbol{P} = \boldsymbol{A}^{\text{T}}\boldsymbol{R}$ is expressed as (14) :

$$\begin{bmatrix} \boldsymbol{a}_{11} & \cdots & \boldsymbol{a}_{r1} & \cdots & \boldsymbol{a}_{m1} \\ \vdots & & \vdots & & \vdots \\ \boldsymbol{a}_{1q} & \cdots & \boldsymbol{a}_{\text{rq}} & \cdots & \boldsymbol{a}_{\text{mq}} \\ \vdots & & \vdots & & \vdots \\ \boldsymbol{a}_{1i} & \cdots & \boldsymbol{a}_{\text{ri}} & \cdots & \boldsymbol{a}_{\text{mi}} \\ \vdots & & \vdots & & \vdots \\ \boldsymbol{a}_{1l} & \cdots & \boldsymbol{a}_{\text{rl}} & \cdots & \boldsymbol{a}_{\text{ml}} \end{bmatrix} \begin{bmatrix} \boldsymbol{r}_{11} & \cdots & \boldsymbol{r}_{1q} & \cdots & \boldsymbol{r}_{1i} & \cdots & \boldsymbol{r}_{1l} \\ \vdots & & \vdots & & \vdots & & \vdots \\ \boldsymbol{r}_{r1} & \cdots & \boldsymbol{r}_{\text{rq}} & \cdots & \boldsymbol{r}_{\text{ri}} & \cdots & \boldsymbol{r}_{\text{rl}} \\ \vdots & & \vdots & & \vdots & & \vdots \\ \boldsymbol{r}_{m1} & \cdots & \boldsymbol{r}_{\text{mq}} & \cdots & \boldsymbol{r}_{\text{mi}} & \cdots & \boldsymbol{r}_{\text{ml}} \end{bmatrix}$$
$$= \left[\boldsymbol{A}_1^{\text{T}}\boldsymbol{R} \quad \cdots \quad \mathbf{A}_q^{\text{T}}\mathbf{R} \quad \cdots \quad \mathbf{A}_i^{\text{T}}\mathbf{R} \quad \cdots \quad \mathbf{A}_l^{\text{T}}\mathbf{R}\right]^{\text{T}} \tag{14}$$

where $\boldsymbol{A}_i = [a_{1i} \cdots a_{\text{ri}} \cdots a_{\text{mi}}]^{\text{T}}$ represents the ith column vector of the residual matrix $\boldsymbol{A}$. The elements of the residual matrix $\boldsymbol{R}$ are mainly divided into three categories: the sample of the original signal, the mixed sample of the original signal and noise, and the sample of the noise.

We use the inner product as the criteria for selecting the support index. So, it is defined as (15).

$$p_k = \| \boldsymbol{P}_k \|_2 = \| \boldsymbol{A}_k^{\text{T}}\boldsymbol{R} \|_2 \tag{15}$$

where $\boldsymbol{P}_k$ is the kth column vector of the matrix $\boldsymbol{P}$. Specifically, p_k represents the maximum vertical projection value of the residual matrix $\boldsymbol{R}$ on the vector $\boldsymbol{A}_k$. When the residual matrix $\boldsymbol{R}$ contains more noise energy, the subspace of the receipt signal will be changed so that the maximum projection on the column vector $\boldsymbol{A}_k$ will be changed accordingly, which can result in an error support index. So, recovery signal obtained by (10) will be wrong due to the mistake support, which can affect the effective sensing about the original signal. From this, when the noise is in higher level, it will seriously affect the recovery of the correct support. Therefore, it is slightly defective to use the CS recovery algorithm directly in MWC.

Based on the above reasons, the RSRA is proposed to reduce the loss of the effective frequency band. Due to $f_p \geq B$, the continuous carrier frequency band is usually distributed in two adjacent spectral slices. Assuming that kth spectral slice and $k+1$th spectral slice contain the efficient continuous carrier frequency band, namely $k, k+1 \in \text{supp}(\boldsymbol{U})$, and the energy about two spectral slices satisfies $E_k > E_{k+1}$. By the (15), we can obtain the maximum inner product $p_{\max} = p_k$, whose column index k is one element of the support. When the noise power is greater than its adjacent carrier signal power, the actual support index $k+1$ will be ignored. So, the adjacent indices k–1 and $k+1$ are added to the support to improve the spectrum sensing performance. However,

© The Institution of Engineering and Technology 2019

Input: measurement matrix **A**, dimensional frame vector **V**, Sparsity N
Output: support S

initialization: residual matrix **R**=**V**, support $S_0=\varnothing$, i=1

1) $p_k=\|\mathbf{P}_k\|_2=\|\mathbf{A}_k^T\mathbf{R}\|_2$, k=1,2,...,L, $\mathbf{A}_k$ is the k-th column of matrix **A**.
2) $z_k = p_k / \|\mathbf{A}_k\|_2$, k=1,2,...,L, and find the largest item in the vector z and assign its index k to λ
3) Compare d_{λ_i-1} and d_{λ_i+1}. Assign the larger subscript to η_i
4) Update $S_i=[S_{i-1},\lambda_i,L+1-\lambda_i,\eta_i,L+1-\eta_i]$, where $L+1-\lambda_i$ is the symmetric support index
5) Evaluate $\hat{\mathbf{U}}_S=\mathbf{A}_{S_i}^{\dagger}\mathbf{R}_{i-1}$
6) Update the residual matrix $\mathbf{R}_i=\mathbf{V}-\mathbf{A}_{S_i}\hat{\mathbf{U}}_S$. $i=i+1$.
7) Determine whether to meet $i>N/2$. If satisfies, then stop iteration. If not satisfies, return to the first step.

Fig. 4 *RSRA algorithm for MWC system*

the addition of the error support index k–1 can increase the noise interference to the spectrum detection. The following will address how to reduce the influence of the error support index.

According to theorem 2 in [11], we can simply get the following, which will be the standard for optimising the later support. Suppose multiband signal $x(t)$ contains N bands, each of which is not exceed B. If $f_s=f_p\ge B$ and $2N\le \mathrm{rank}(\boldsymbol{A})\le m$. Then, the support satisfies $|\mathrm{supp}(\boldsymbol{Z}(f))|\le 2N$. Here, $\mathrm{supp}(\boldsymbol{Z}(f))=\mathrm{supp}(\boldsymbol{U})$.

It specifies the number of MWC recovery support. If $|\mathrm{supp}(\mathbf{Z}(f))|\ge 2N$, there will exist one carrier band taking up three continuous spectrum slices simultaneously. However, this will go against the condition $f_s=f_p\ge B$ when the signal contains N bands. So the support must satisfy $|\mathrm{supp}(\mathbf{Z}(f))|\le 2N$, that is, a wideband signal with N carrier bands has up to $2N$ support indexes that contain the valid information about the signal.

In order to filter the effective support, the support correlation coefficient matrix $\boldsymbol{D}_{i,j}$ is defined to measure the distribution of the signal bands in each slice of the spectrum. The expression is as follows:

$$\boldsymbol{D}_{i,j}=\frac{\sum_{j=1}^{p}\sum_{i=1}^{q}(\boldsymbol{A}_j-\bar{\boldsymbol{A}})(\boldsymbol{Y}_i-\bar{\boldsymbol{Y}})}{\sqrt{\sum_{j=1}^{p}(\boldsymbol{A}_j-\bar{\boldsymbol{A}})^2}\sqrt{\sum_{i=1}^{q}(\boldsymbol{Y}_i-\bar{\boldsymbol{Y}})^2}} \tag{16}$$

where $\boldsymbol{A}_j$ is the jth column vector of the matrix $\boldsymbol{A}$. $\boldsymbol{Y}_i$ is the ith column vector of the sampling matrix $\boldsymbol{Y}$. p represents the total number of columns of the measurement matrix $\boldsymbol{A}$, and q is the number of columns of the matrix $\boldsymbol{Y}$.

$$d_k=\|\boldsymbol{D}_k\|_2,\ k=1,2,\ldots,p \tag{17}$$

where $\boldsymbol{D}_k$ is the kth column vector of the matrix $\boldsymbol{D}$. d_k denotes the correlation between the signal subspace vector and the vector $\boldsymbol{A}_k$. The effective support k obtained by formula (15) makes the signal subspace vector have a large correlation with the vector $\boldsymbol{A}$. However, the addition of noise will reduce this correlation easily. Therefore, the relationship between the subspace vector and the vector $\boldsymbol{A}_k$ can be amplified by the formula (17), and the adjacent support index with large correlation can be selected as the effective frequency band to improve the recognition rate of the support. So, the proposed algorithm that reconstructs the support is as follows (Fig. 4).

By adding the valid adjacent support index in step 3, four support indexes are obtained in each iteration. The algorithm not only improves the anti-noise performance but also reduces the number of iterations by half.

4 Numerical experiments

In the electromagnetic spectrum sensing scene, MWC only needs to reconstruct the frequency domain support S to achieve the target of spectrum sensing. As long as the S is accurately obtained, the result of the spectrum sensing must be reliable. The Monte–Carlo simulations (MCs) are used to calculate the reconstruction probability Pr of the support S as following:

$$P_r=\frac{S_r}{N_t} \tag{18}$$

where S_r is the number of successful reconstruction simulations, and N_t is the total number of the MCs. The time domain signal model used in the comparison experiments was as follows:

$$x(n)=\sum_{i=1}^{N}\sqrt{E_iB}\sin c(\mathrm{B}(n-\tau_i))\cos(2\pi \mathrm{f}_i(n-\tau_i)) \tag{19}$$

where energy coefficient $E_i=\{1,2,3\}$, time delay $\tau_i=\{0.4,0.7,0.2\}\mu$s, $f_{\mathrm{NYQ}}=10\,\mathrm{GHz}$, sampling frequency $f_s=f_p=f_{\mathrm{NYQ}}/195\simeq 51.3\,\mathrm{MHz}$. The length of the signal generated by (19) is 19,695, and $L=195$. So the length of our observation sampled from sampling channels is 101 (19695/195).

In order to reflect the anti-noise performance, White Gaussian noise is added to the original signal. We set SNR = 5 dB. After low-pass filtering and low-speed sampling, the original signal was recovered by RSRA.

To prove the idea in Section 3, Fig. 5 shows the correlation between each column vector of the measurement matrix and the sampling matrix under the various SNR conditions. X in the figures represents the position of the correct support, and Y represents the degree of relevance. The simulations in Fig. 5 demonstrate that one carrier frequency band is usually distributed in two consecutive spectrum slices, and the measurement matrix column vectors corresponding to the support indices are greatly related to the sampling data. In addition, as shown in Fig. 5*b* with $X=36$ and $X=160$, the correlation of its adjacent valid support index $X=35$ and $X=161$ are still higher than the correlation of another adjacent index 37 and 159 although the noise has great impact on it. Therefore, this correlation can be used as the standard for screening effective support.

Fig. 6 shows the time domain and frequency domain of the original signal, and Fig. 7 shows the time domain and frequency domain of the recovery signal. The simulation results demonstrate that RSRA is feasible completely for the MWC framework, and the recovery effect of the RSRA algorithm is ideal in time domain and frequency domain.

The following experiences examine the influence of SNR on recovery performance. One thousand MC experiments were performed under the same conditions to calculate the reconstruction rate of the support. The simulations demonstrate that our algorithm outperforms the other algorithms in Fig. 8 as expected, especially in low SNR. This is due to the fact that correlation calculation plays a significant role in the support index selection. Under the same recovery rate, our algorithm can reduce 5 dB to obtain the same perception effect compared to MMV-OMP algorithm. Moreover, when the curves become flat in Fig. 8, MMV-OMP and IOMP will go beyond the RSRA algorithm slightly. This is because the correlation between the column vectors of the measurement matrix and the sampling matrix cannot work well when the noise is in low level. This will result in the misjudgment of support recovery. Fortunately, this problem a small probability event, and can be solved by adding the number of channels.

To examine the effect of the sparsity on recovery performance, we simulated the effect of band number on recovery rate. We set SNR = 20 and $m=50$. When the number of bands increases, the recovery rate will be reduced due to the restriction of the channels' number. As shown in Fig. 9, the advantage of our algorithm is that

© The Institution of Engineering and Technology 2019

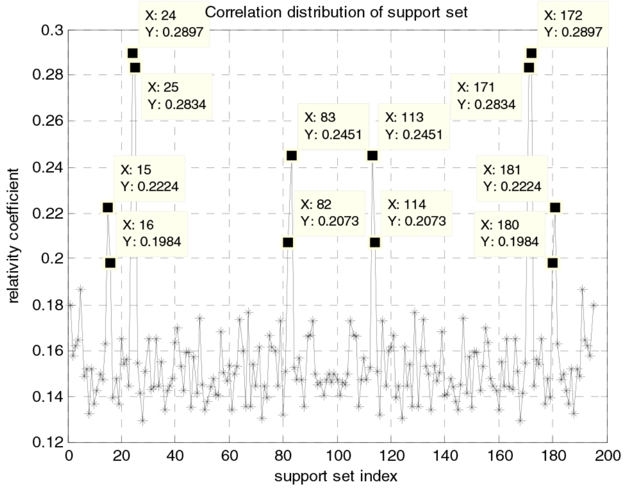

a

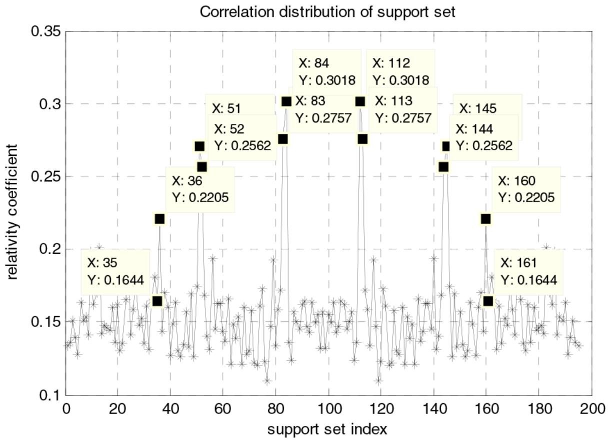

b

Fig. 5 *Correlation distribution graph of Support*
(a) SNR = 10 dB, $N = 6$, ***(b)*** SNR = 5 dB, $N = 6$

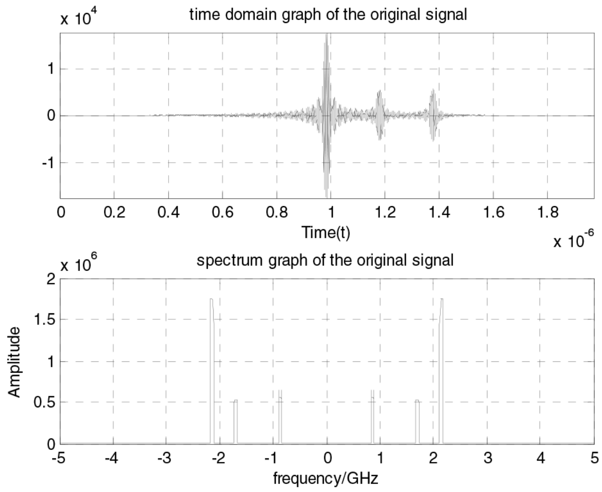

Fig. 6 *Original signal and its spectrum*

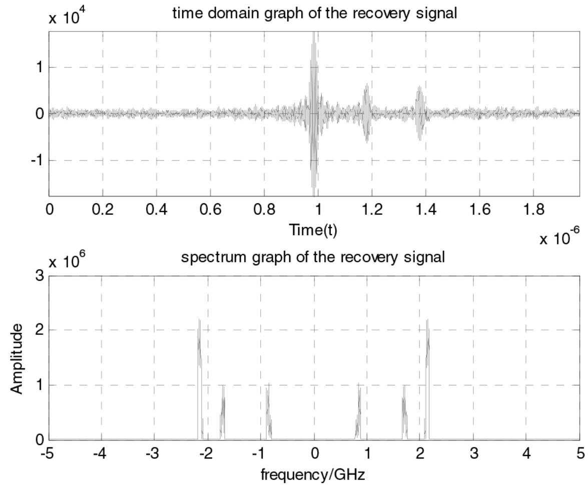

Fig. 7 *Reconstructed signal based on SRSA and its spectrum*

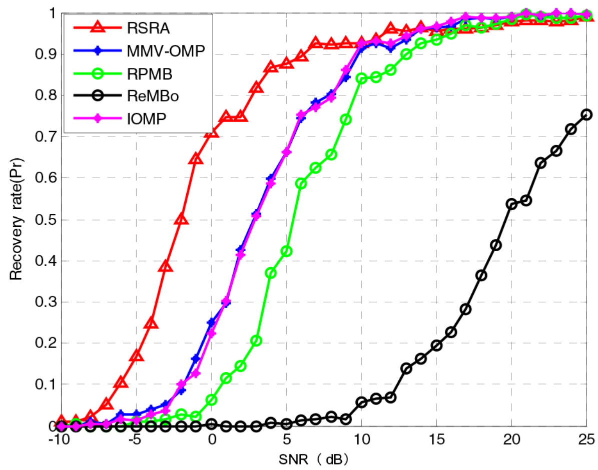

Fig. 8 *Percentage of support recovery under different SNR levels*

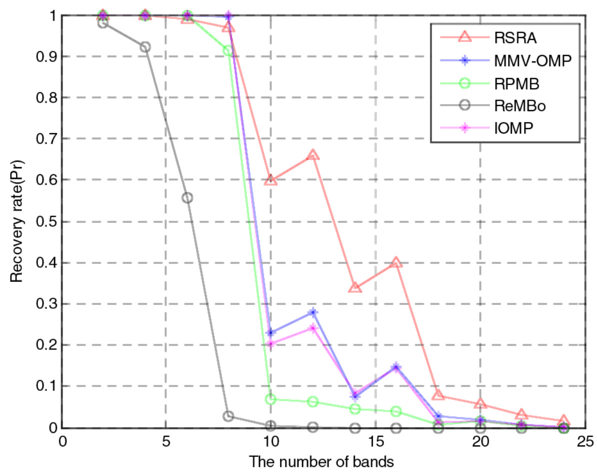

Fig. 9 *Percentage of support recovery with different number of signal bands*

it can improve the recovery rate when the number of sub-bands become large. The more the sub-bands, the more obvious the effects. It is because that our recovery algorithm makes full use of the correlation between the random moving spectrum slices. When the number of frequency bands increases to a certain degree, the accuracy of perception is particularly low. The signal sampled by MWC system must satisfy the sparse property, which is the reason that causes the perception result to decline. So, the perception accuracy can be improved by increasing the number of channels.

In addition, the channel number is an important factor that restricts the recovery of sparse signal. In order to track the influence of channel number on recovery performance, we reduce the influence of noise which is given with SNR = 30. Fig. 10 depicts that the proposed algorithm RSRA is slightly higher than other algorithms when small number of channels participate in the spectrum sensing. The less the signal sub-band, the less the number of channels required for completely recovery. While ensuring anti-noise performance, our algorithm can also reduce the number of channels. The simulations indicate that the proposed algorithm can enhance the robust for the recovery performance of MWC.

In order to intuitively reflect the time complexity of the proposed algorithm, the experiment compares the average recovery

© The Institution of Engineering and Technology 2019

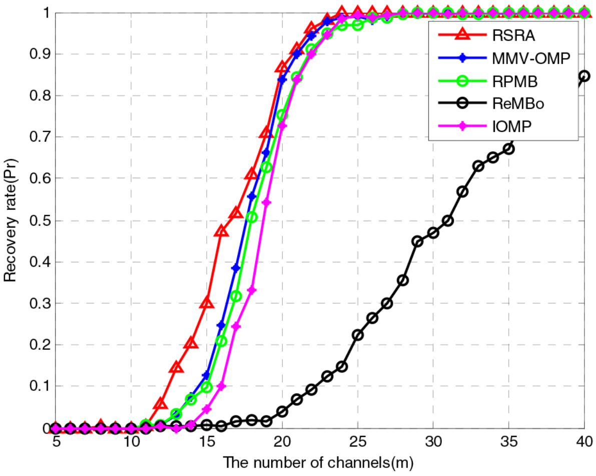

Fig. 10 *Percentage of support recovery under different number of channels*

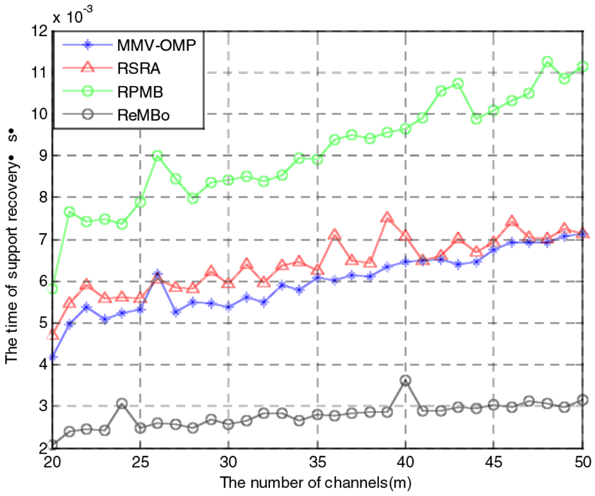

Fig. 11 *Support recovery time under different number of channels*

time of the four reconstruction algorithms. Fig. 11 shows that ReMBo has the lowest time complexity, but its recovery performance is the worst. In addition, the complexity of our proposed algorithm RSRA is slightly higher than that of MMV-OMP. However, RSRA has higher recovery performance than MMV-OMP in all aspects, especially at low SNR situation. The running time of RSRA is up to 1 ms more than MMV-OMP, so the difference between RSRA and MMV-OMP in terms of time complexity is within acceptable range. It can be seen that the proposed algorithm has good real-time performance and anti-noise performance in realising spectrum sensing.

5 Conclusions

In order to improve the anti-noise performance for the support recovery, this paper proposes a RSRA in modulated wideband converter for spectrum sensing. To explore the relationship between support indexes, we simulate the correlation distribution between the column vectors of the measurement matrix and the sampling matrix. Experiments show that the correlation between the adjacent effective support is stronger, so the recovery rate of the support can be improved by selecting the higher correlation between the two adjacent support indexes. The results show that the recovery rate of the RSRA algorithm in lower SNR is higher than that of the other methods. Therefore, the spectrum sensing in the relatively poor noise environment can be achieved efficiently by RSRA.

6 Acknowledgments

This work was supported by the Science and Technology Plan Project of Sichuan Province in China, named Security Collaborative Spectrum Sensing Network Based on The MWC System (No.2016GZ0091).

7 References

[1] Wu, J., Yang, D., Chen, Z.: 'Design and application of multi-stage reconfigurable signal processing flow on FPGA', *Comput. Electr. Eng.*, 2015, **42**, pp. 1–11

[2] Chen, T., Li, P., Zhang, W., *et al.*: 'A novel channelized FB architecture with narrow transition bandwidth based on CEM FRM', *Ann. Telecommun.*, 2016, **71**, (1), pp. 27–33

[3] Lin, Y.P., Vaidyanathan, P.: 'Periodically nonuniform sampling of bandpass signals', *IEEE Trans. Circuits Syst. Ii-Analog Digit. Signal Process.*, 1998, **45**, (3), pp. 340–351

[4] Donoho, D.L.: 'Compressed sensing', *IEEE Trans. Inf. Theory*, 2006, **52**, (4), pp. 1289–1306

[5] Candès, E.J., Romberg, J., Tao, T.: 'Robust uncertainty principles: exact signal reconstruction from highly incomplete frequency information', *IEEE Trans. Inf. Theory*, 2006, **52**, (2), pp. 489–509

[6] Anitori, L., Maleki, A., Otten, M., *et al.*: 'Design and analysis of compressed sensing radar detectors', *IEEE Trans. Signal Process.*, 2016, **61**, (4), pp. 813–827

[7] Stinco, P., Greco, M.S., Gini, F.: 'Spectrum sensing and sharing for cognitive radars', *IET Radar Sonar Navig.*, 2015, **10**, (3), p. pp. 595–602

[8] Fang, B., Huang, G., Gao, J.: 'Sub-nyquist sampling and reconstruction model of LFM signals based on blind compressed sensing in FRFT domain', *Circuits. Syst. Signal Process.*, 2015, **34**, (2), pp. 419–439

[9] Tropp, J.A., Laska, J.N., Duarte, M.F., *et al.*: 'Beyond nyquist: efficient sampling of sparse bandlimited signals', *IEEE Trans. Inf. Theory*, 2010, **56**, (1), pp. 520–544

[10] Xu, L., Ren, Y., Sun, S., *et al.*: 'Compressive sensing-based wideband capacitance measurement with a fixed sampling rate lower than the highest exciting frequency', *Meas. Sci. Technol.*, 2016, **27**, (3), p. 035006

[11] Mishali, M., Eldar, Y.C.: 'From theory to practice: sub-nyquist sampling of sparse wideband analog signals', *IEEE. J. Sel. Top. Signal Process.*, 2010, **4**, (2), pp. 375–391

[12] Mishali, M., Eldar, Y.C.: 'Blind multiband signal reconstruction: compressed sensing for analog signal', *IEEE Trans. Signal Process.*, 2009, **57**, (3), pp. 993–1009

[13] Mishali, M., Eldar, Y.C.: 'Reduce and boost: recovering arbitrary sets of jointly sparse vectors', *IEEE Trans. Signal Process.*, 2008, **56**, (10), pp. 4692–4702

[14] Gai, J.X., Fu, P., Sun, J.Y., *et al.*: 'A recovery algorithm of MWC sub-nyquist sampling based on random projection method', *Acta Electron. Sin.*, 2014, **42**, (9), pp. 1686–1692

[15] Jia, M., Shi, Y., Gu, X.M., *et al.*: 'Improved algorithm based on modulated wideband converter for multiband signal reconstruction', *Eurasip J. Wirel. Commun. Netw.*, 2016, **2016**, (1), p. 50

[16] Zhang, R.Y., Zhao, H.L., Jia, S.B., *et al.*: 'Sparse multi-band signal recovery based on support refining for modulated wideband converter'. IEEE Int. Conf. Signal Processing, Chengdu, China, 2017, pp. 304–309

[17] Yu, N., Qi, X.H., Qiao, X.L.: 'Multi-channels wideband digital reconnaissance receiver based on compressed sensing', *IET Signal Process.*, 2013, **7**, (8), pp. 1367–1375

[18] Xu, Z.Y., Li, Z., Li, J.: 'Broadband cooperative Spectrum sensing based on distributed modulated wideband converter', *Sensors*, 2016, **16**, (10), p. 1602

[19] Stein, S., Yair, O., Cohen, D., *et al.*: 'CaSCADE: compressed carrier and DOA estimation', *IEEE Trans. Signal Process.*, 2017, **65**, (10), pp. 2645–2658

[20] Lv, W., Wang, H., Mu, S.: 'Spectrum sensing using co-prime array based modulated wideband converter', *Sensors*, 2017, **17**, (5),, p. 1052

© The Institution of Engineering and Technology 2019